

# A Trajectory Tracking Control of a Skid Steered Mobile Cleaning Robot

Seungwoo Jeon<sup>1</sup>, Wootae Jeong<sup>2</sup>, Soon-Bark Kwon<sup>2</sup>, Cheulkyu Lee<sup>2</sup> and Duckshin Park<sup>2</sup>

<sup>1</sup>Department of Robotics & Virtual Engineering, Korea University of Science and Technology, Daejeon, Korea

<sup>2</sup>Transportation Environmental Research Team, Korea Railroad Research Institute, Gyeonggi-do, Uiwang, Korea

Keywords: Mobile Platform, Four Wheel Skid Steering, Trajectory Tracking, Mass Center.

Abstract: Cleaning accumulated dusts inside air ventilation ducts of underground facilities is an essential process to improve indoor air quality, especially at the underground facilities such as subway platforms. Therefore, various autonomous mobile duct cleaning robots have been actively studied to be applied at the closed space of the ventilation duct. In this paper, the four wheeled skid steering mobile platform with rotating brush-arms has been developed and proposed an effective skid steering control technique under changeable center of mass (CM) of the platform. The shifted CM of the platform and unstable disturbances acting on the rotating brushes from cleaning surfaces can change the dynamic steering characteristics of the platform. Therefore, this paper also proposes a new integrated backstepping and I-PD controller for stable trajectory tracking of the platform and proves the effects of the controller through simulations.

## 1 INTRODUCTION

HVAC ducts have to be cleaned regularly to improve indoor air quality that can affect the health of people. The mechanical brushing method was reported as the most efficient duct cleaning method among various duct cleaning methods (Holopainen *et al*, 2003). Nevertheless, the most of air ventilation ducts at many industrial facilities has been still cleaned by the human. To increase efficiency and safety in cleaning inside air ducts, various autonomous duct cleaning technologies have been suggested by using mobile platforms (Jeon *et al*, 2013).

The autonomous mobile cleaning robot without steering system requires skid-steering technique for trajectory-tracking control. Since the skid-steering uses the velocity difference between two wheels, the platform can be modelled with a non-holonomic constraint based on the specific kinematic and dynamic characteristics (Caracciolo *et al*, 1999). However, the singularity problem can be occurred at pivot-turning: the velocity at the center of mass(CM) becomes zero. To avoid the singularity problem from the estimated dynamic model, a backstepping technique was used to provide feedback for the current velocity of the platform equipped with steering mechanism (Fierro *et al*, 1997). Tracking

error should be minimized to increase pressurizing force for the brush to the workspace (Jeong *et al*, 2012).

However, the CM of the platform is also changeable by reciprocating motion of the upper brush-arm and dynamic disturbances occurred from nonlinear friction between brush and duct surface make the tracking error increase. These trajectory tracking errors can be reduced by applying an additional neural-network controller with a fully unattainable parameter such as a friction coefficient between wheel and the floor of ducts(Fierro *et al*, 1997). However, implementing the training process of a neural-network or adaptive logic requires a high speed processor and long computational time (Kim *et al*, 2006).

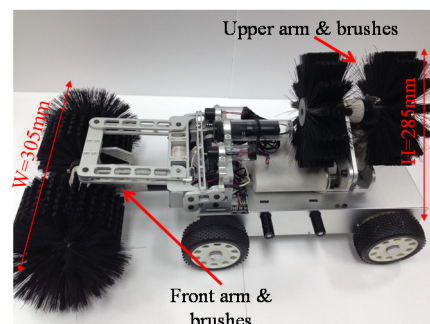


Figure 1: Prototype of the duct cleaning robot.

In this paper, a simple and robust control method is proposed to enable the stable trajectory tracking of the duct cleaning robot to reduce the effect of uncertainties occurred by shifting CM of the platform.

Figure 1 shows the prototype of the duct cleaning robot which has two robotic arms and rolling brushes for cleaning inside duct.

## 2 DYNAMIC ANALYSIS

### 2.1 Modelling of the Mobile Platform

For the trajectory tracking control of the mobile platform, a mathematical model of the platform was presented by considering both kinematic and dynamic characteristics. As depicted in Figure 2, the fixed coordinate system was set to  $q=[X, Y, \phi]$ , the posture angle,  $\phi$ , of the platform was the same as the yaw angle, and the moving coordinate system  $[x, y, \phi]$  was defined to be placed at the center of mass (CM) of the platform. The wheel slip was neglected.

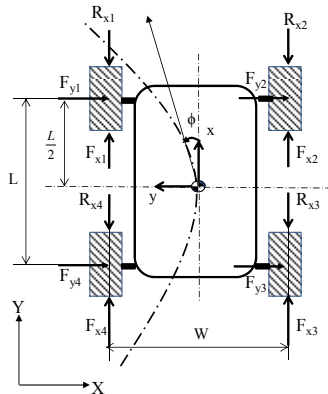


Figure 2: A schematic model of the mobile platform.

Based on the schematic model of the mobile platform illustrated in Figure 2, the equation of motion of the platform can be given by Example:

$$\begin{aligned} m\ddot{x} &= \sum_{i=1}^4 F_{xi} - \sum_{i=1}^4 R_{xi} + m\dot{y}\dot{\phi}, \\ m\ddot{y} &= -\sum_{i=1}^4 F_{yi} + m\dot{x}\dot{\phi}, \\ I\ddot{\phi} &= W(F_{x1} - F_{x2}) - M_r. \end{aligned} \quad (1)$$

where  $F_{xi}$  is the tractive force at the contact point of the wheel,  $R_{xi}$  is the longitudinal resistive force of the wheel,  $F_{yi}$  is the lateral force at the contact point of the wheel (Caracciolo *et al*, 1999). By assigning

friction coefficients ( $\mu_x, \mu_y$ ) as a constant, the resistive force, lateral force, and resistive moment at the CM can be calculated as

$$R_x = \sum_{i=1}^4 R_{xi} = \mu_x \frac{mg}{4} \sum_{i=1}^4 \text{sgn}(\dot{x}_i), \quad (2)$$

$$F_y = \sum_{i=1}^4 F_{yi} = \mu_y \frac{mg}{L} (\text{sgn}(\dot{y}_1) + \text{sgn}(\dot{y}_3)), \quad (3)$$

$$\begin{aligned} M_r &= \frac{L}{2} (F_{y1} + F_{y2} - F_{y3} - F_{y4}) \\ &+ \frac{W}{2} (R_{x2} + R_{x3} - R_{x1} - R_{x4}). \end{aligned} \quad (4)$$

The dynamic model of the platform with generalized coordinates,  $q=(X, Y, \phi)$  can be expressed as a matrix form by

$$\begin{aligned} \mathbf{M}\ddot{\mathbf{q}} &= \mathbf{E}(\mathbf{q})\boldsymbol{\tau} - \mathbf{F}(\mathbf{q}, \dot{\mathbf{q}}) \\ \mathbf{M} &= \begin{pmatrix} m & 0 & 0 \\ 0 & m & 0 \\ 0 & 0 & I \end{pmatrix}, \quad \mathbf{F}(\mathbf{q}, \dot{\mathbf{q}}) = \begin{bmatrix} R_x \cos \phi - F_y \sin \phi \\ R_x \sin \phi + F_y \cos \phi \\ M_r \end{bmatrix}, \\ \mathbf{E}(\mathbf{q}) &= \frac{1}{r} \begin{pmatrix} \cos \phi & \cos \phi \\ \sin \phi & \sin \phi \\ W/2 & -W/2 \end{pmatrix}, \quad \boldsymbol{\tau} = 2rF_{xi} (i=1,2), \end{aligned} \quad (5)$$

where  $r$  is the wheel radius,  $\boldsymbol{\tau}$  are the torques at left and right side of motors to drive wheels. To accomplish the skid steering by creating a differential velocity between left and right side of wheels, the kinematic equation concerning about the platform velocity,  $\mathbf{v}$ , can be written by

$$\dot{\mathbf{q}} = \mathbf{S}(\mathbf{q})\mathbf{v}, \quad \mathbf{v} \in \mathbb{R}^2 \quad (6)$$

$$\mathbf{S}(\mathbf{q}) = \begin{bmatrix} \cos \phi & 0 \\ \sin \phi & 0 \\ 0 & 1 \end{bmatrix}, \quad (7)$$

where  $\mathbf{v} = [v_{linear}, v_{angular}]^T = [v_1, v_2]^T$  refers to the linear and angular velocity vector at the CM and  $\mathbf{S}(\mathbf{q})$  is  $3 \times 2$  matrix for coordinate transformation.

Since front and rear wheels are directly connected with V-belts, the four-wheel skid-steering platform can be considered as a two-wheel differential driven mobile platform (Martinez *et al*, 2005). The equation of motion for the platform with nonholonomic constraint can be presented as

$$\begin{aligned} \mathbf{M}\ddot{\mathbf{q}} &= \mathbf{E}(\mathbf{q})\boldsymbol{\tau} + \mathbf{A}^T(\mathbf{q})\boldsymbol{\lambda} - \mathbf{F}(\mathbf{q}, \dot{\mathbf{q}}) \\ &= \mathbf{E}(\mathbf{q})\boldsymbol{\tau} - \mathbf{F}(\mathbf{q}, \dot{\mathbf{q}}), \\ \therefore \mathbf{A}(\mathbf{q})\dot{\mathbf{q}} &= [-\sin \phi \quad \cos \phi \quad 0] \begin{bmatrix} \dot{X} \\ \dot{Y} \\ \dot{\phi} \end{bmatrix} = 0 \end{aligned} \quad (8)$$

From the Equation (6) and Equation (8), the state feedback control law becomes

$$\boldsymbol{\tau} = (\mathbf{S}^T \mathbf{E})^{-1} (\mathbf{S}^T \mathbf{M} \mathbf{S} \mathbf{u} + \mathbf{S}^T \mathbf{M} \dot{\mathbf{S}} \mathbf{v} + \mathbf{S}^T \mathbf{F}), \quad (9)$$

where  $\mathbf{u} = \dot{\mathbf{v}} = [\dot{v}_1, \dot{v}_2]$  refers to the control input.

As the platform moves, the upper brush arm on the mobile platform makes duct surface cleaned by reciprocating mechanism. The CM of the platform can be shifted by the motion of the upper brush arm. Consequently, the yaw moment of the platform can be changed. Therefore, for trajectory tracking control, steering commands calculated by torques of traction motors have to be determined by considering the dynamic shifts of the CM (see Figure 3).

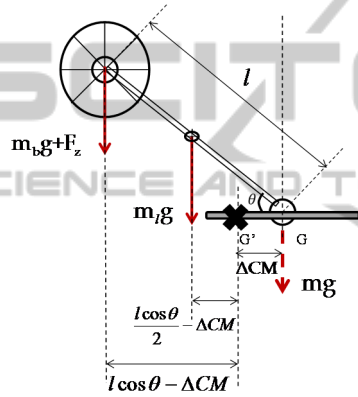


Figure 3: Simplified model of the upper rotating brush arm.

The shifting position of the CM can be calculated as

$$\Delta CM = \frac{m_b}{m} L_x, \quad L_x = l \cos \theta, \quad (10)$$

where  $l$  is the length of the brush arm,  $\Delta CM$  is a shifted distance of the CM in the lateral direction,  $m_b$  is the mass of the rotating brush, and  $m$  is the overall mass except the brush and arm. The rotation angle of the brush arm,  $\theta$ , ranges from 0 to 180 [deg] as shown in Figure 3. As the CM changes, the yaw moment of the platform is changed. Thus, the resistive moment of the Equation (4) can be recalculated as follows

$$\begin{aligned} W_L &= \frac{W}{2} - \Delta CM, \quad W = W_R + W_L, \\ M_r &= \frac{L}{2} (F_{y1} + F_{y2} - F_{y3} - F_{y4}) \\ &\quad + W_R (R_{x2} + R_{x3}) - W_L (R_{x1} + R_{x4}) \end{aligned} \quad (11)$$

By considering the shifted CM position as depicted in Figure 4, the yaw moment change and velocity

changes are required for accurate steering control of the platform.

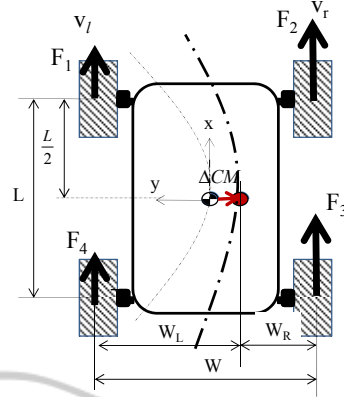


Figure 4: A scheme of skid-steering motion with the shifting center of mass (CM) of the platform.

## 2.2 Trajectory Tracking Control

In order to control the platform as a given trajectory, dynamic uncertainties by the CM position changes and rubbing force by brush-arm need to be considered to determine the control inputs and motor torques. Additionally, the tracking control has to be designed to make the pivot-truning which can cause uncontrollable with zero velocity at the CM.

Therefore, The *integrator backstepping method* can be applied with incomplete dynamic model of the nonholonomic system. The error vector,  $\mathbf{e}$ , between the target point on the given trajectory and the platform location and the differential vector of the error vector can be expressed as

$$\begin{aligned} \mathbf{e} &= \mathbf{T}(\mathbf{q}_r - \mathbf{q}), \\ \mathbf{e} &= \begin{bmatrix} e_x \\ e_y \\ e_\phi \end{bmatrix} = \begin{bmatrix} \cos \phi & \sin \phi & 0 \\ -\sin \phi & \cos \phi & 0 \\ 0 & 0 & 1 \end{bmatrix} \begin{bmatrix} X_r - X \\ Y_r - Y \\ \phi_r - \phi \end{bmatrix}, \\ \dot{\mathbf{e}} &= \begin{bmatrix} -v_1 + v_2 e_y + \dot{x}_r \cos(e_\phi) \\ -v_2 e_x + \dot{x}_r \sin(e_\phi) \\ \dot{\phi}_r - v_2 \end{bmatrix}. \end{aligned} \quad (12)$$

The derivative of the platform target velocity,  $\dot{v}_c$ , for trajectory tracking can be calculated as

$$\begin{aligned} \mathbf{v}_c &= \begin{bmatrix} \dot{x}_r \cos(e_\phi) + k_1 e_x \\ \dot{\phi}_r + k_2 x_r e_y + k_3 x_r \sin(e_\phi) \end{bmatrix}, \\ \dot{\mathbf{v}}_c &= \begin{bmatrix} \ddot{x}_r \cos(e_\phi) \\ \ddot{\phi}_r + k_2 \dot{x}_r e_y + k_3 \dot{x}_r \sin(e_\phi) \end{bmatrix} \\ &\quad + \begin{bmatrix} k_1 & 0 & -\dot{x}_r \sin(e_\phi) \\ 0 & k_2 \dot{x}_r & k_3 \dot{x}_r \cos(e_\phi) \end{bmatrix} \dot{\mathbf{e}}. \end{aligned} \quad (13)$$

where  $\dot{v}_c$  can be applied to the concept of the *perfect velocity tracking* to obtain the control input expressed in Equation (9). However, it is infeasible for an actual platform to be controlled at a target velocity without feedback of velocity errors in the trajectory tracking. Therefore, the control input can be expressed with feedback of the platform velocity as follows

$$\mathbf{u} = \dot{\mathbf{v}}_c + \mathbf{K}_4(\mathbf{v}_c - \mathbf{v}), \quad (14)$$

where  $\mathbf{K}_4$  can be a positive definite, diagonal matrix  $\mathbf{K}_4 = k_4 \mathbf{I}$ .

Additionally, using the Lyapunov function, the error vector ( $\mathbf{e}$ ) of Equation (12) can asymptotically converge to zero value as proven by (Fierro *et al.*, 1997). Nevertheless, when dynamic uncertainties are occurred by shifting CM and the pressurizing force applied by the brush-arm, stability of the trajectory tracking cannot be assured. To obtain additional control input for reducing the position error, simple PID controller can be adopted. However, the traction motor can be damaged by the derivative (D) controller which magnifies the input signal with disturbances. Thus, a digital I-PD controller, whose proportional(P) and derivative(D) controller are feedbacked by actual measurement values, can be implemented by placing low pass filter in front of D controller (King *et al.*, 2010).

Figure 6 shows the control flow scheme integrating the Backstepping method and the I-PD controller for trajectory tracking control of the platform. The I-PD controller can be converted to discrete form and expressed as Equation (15). The new control input can be obtained by integrating the I-PD controller and the Backstepping controller of the velocity, as expressed in Equation (16)

$$\begin{aligned} \mathbf{u}_{PID,k} &= \mathbf{u}_{PID,k-1} + \Delta \mathbf{u}_{PID,k}, \\ \Delta \mathbf{d}_k &= (\eta \cdot \beta - 1) \mathbf{d}_{k-1} + \beta (\mathbf{e}_k - \mathbf{e}_{k-1}), \\ \mathbf{d}_k &= \mathbf{d}_{k-1} + \Delta \mathbf{d}_k, \end{aligned} \quad (15)$$

$$\begin{aligned} \Delta \mathbf{u}_{PID,k} &= k_p \left[ (\mathbf{e}_k - \mathbf{e}_{k-1}) + \frac{\Delta t}{T_i} \times \mathbf{e}_k + \Delta \mathbf{d}_k \right], \\ \mathbf{u}' &= \dot{\mathbf{v}}_c + \mathbf{K}_4(\mathbf{v}_c - \mathbf{v}) + \mathbf{u}_{PID,k}, \end{aligned} \quad (16)$$

where derivative gain is  $1/\eta = 10$ , effective D-gain ( $\beta$ ) is  $T_d / (\Delta t + \eta \cdot T_d)$ ,  $\mathbf{e}_k$  is position error at X and Y coordinates,  $\mathbf{e}_{k-1}$  is position error in a previous sampling period,  $k_p$  is proportional gain,  $T_i$  is time integration,  $T_d$  is time derivative, and  $\Delta t$  is a sampling time. Since input value ( $\mathbf{u}_{PID}$ ) of the I-PD controller is calculated by the previous sampling time, sudden changes at input signal can be

prevented. In addition, the  $\mathbf{d}_k$  term is a derivative controller with low-pass filter as a discrete form.

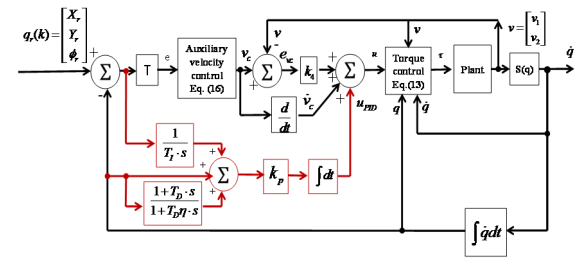


Figure 5: A control scheme for the suggested trajectory tracking control.

### 3 SIMULATION RESULTS

For Based on the analytical model of the controller, the simulation of trajectory tracking control was carried out with a MATLAB tool. The parameters of the model were set as: length ( $L=0.3$ [m]), distance from the CM to the front wheel or rear wheel ( $L/2=0.15$ [m]), distance between the left and right wheels ( $w=0.23$ [m]), wheel radius ( $r=0.05$ [m]), mass moment of inertia ( $I=0.19$ [kgm<sup>2</sup>]), total mass of the cleaning robot ( $m_{overall} = 7.823$ [kg]), and top surface tool mass ( $m_{brush} + m_{jink} = 1.777$ [kg]). To consider the pressing effect of the brush arm under unknown friction, a random function within a 20 percentage of pressurizing force has been applied to the wheel of the platform model as a disturbance input. The reference trajectory was constructed as  $x_r = v_r t, y_r = 0.5 \sin(2\pi t / 60)$  to investigate the tracking performance in steering movements. The gains of the backstepping controller can be achieved through iterative computation as  $k_1=9, k_2=40, k_3=0, \mathbf{K}_4 = \begin{bmatrix} 20 & 0 \\ 0 & 20 \end{bmatrix}$  and the gains of the I-PD controller

were set to  $k_p=12, T_i=2.3, T_d=3$ . The initial location of the platform was set to the starting point of the reference path. The reciprocated cleaning movement of the upper brush arm had considered as periodic motion. Figure 6(a) and 6(b) show the position errors and the velocity errors of the platform during the simulation time. The steady state errors have been achieved by applying the Backstepping control. On the other hand, the steady state error has been reduced by integrating I-PD and backstepping controller. From Figure 6(c), the posture angle becomes stable after temporary wobbling motion. As the radius of curvature is decreased, higher torque difference has to be exerted at both sides of platform motors. Therefore, as resulted in Figure 6(d), the

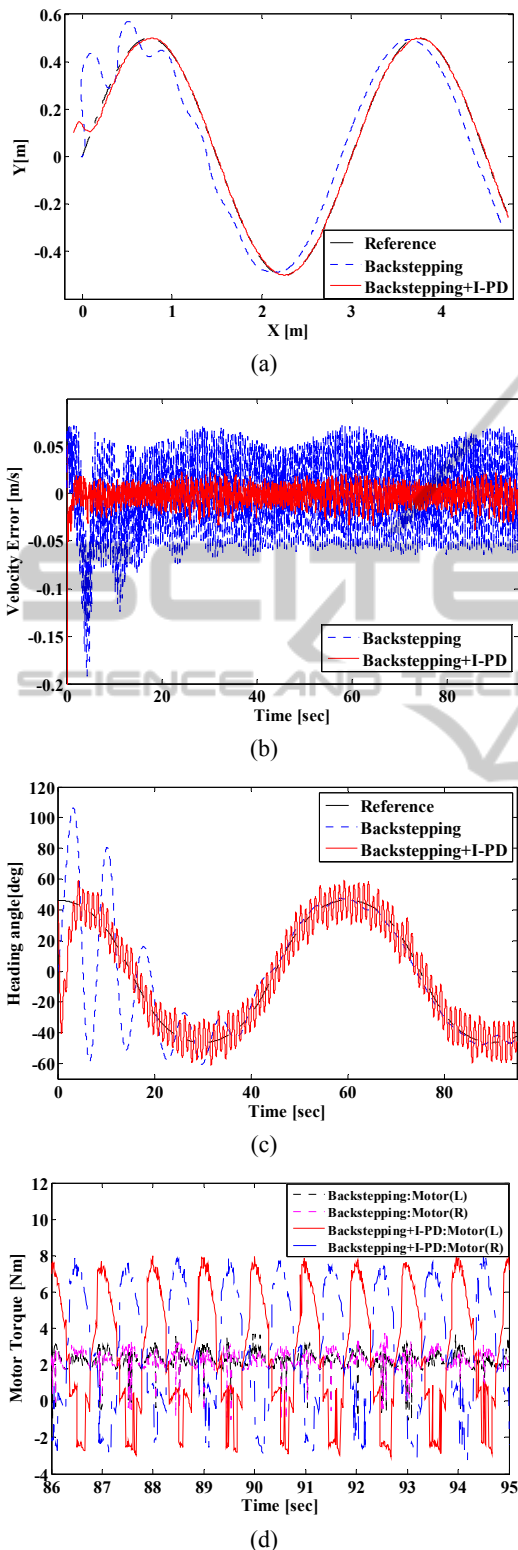


Figure 6: Simulation results with a curved line trajectory tracking, (a) Trajectory, (b) Error in velocity, (c) Posture angle, and (d) Input motor torque.

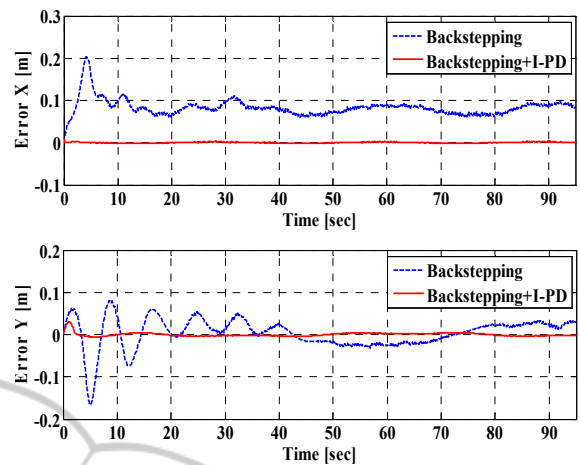


Figure 7: Error comparison in the curved line trajectory tracking.

torque difference at each motor can be generated by exerting resistive torques to create yaw moment of the platform. Figure 7 compares position errors of backstepping controller with integrated I-PD controller with backstepping.

## 4 CONCLUSIONS

A new controller that enables stable trajectory tracking of an autonomous mobile platform for duct cleaning has been presented. Four-wheeled skid steering platform can be confronted by the singularity problem during pivot turning where the velocity at CM of the platform approaches zero. In particular, shifting CM by reciprocating the brush-arm periodically makes the steering moment of the platform change. To avoid singularity problem backstepping technique has been adopted for assigning the estimated target velocity. Nevertheless, under dynamic pressure changes in the brush arm, there existed steady state errors which can not be ignored. Therefore, by integrating a relatively simple I-PD controller with the backstepping, the overall position errors could be reduced, which enables stable trajectory tracking control under variable CM.

## ACKNOWLEDGEMENTS

This research was carried out as a part of project partially funded by the Ministry of Land, Infrastructure and Transport and Ministry of Science, ICT and Future Planning in Korea.

## REFERENCES

- Holopainen, R., Asikainen, V., Tuomainen, M., Bjorkroth, M., Pasanen, P., Seppanen, O., 2003. Effectiveness of duct cleaning methods on newly installed duct surfaces. *Indoor Air*. Vol. 13: pp.212-222.
- Jeon, S., Jeong, W., Park, D., 2013. Surface Cleaning Force Control of Rotating Brushes For an Air Duct Cleaning Robot, *International Conference on Informatics in Control, Automation and Robotics (ICINCO), 2013 July 29-31; Reykjavik, Iceland*. pp. 453-457. SCITEPRESS.
- Caracciolo, L., De Luca, A., Iannitti, S., 1999. Trajectory Tracking Control of a Four-Wheel Differentially Driven Mobile Robot. *IEEE International Conference on Robotics and Automation*. 1999 May 10-15; Detroit, MI. pp. 2632-2638.
- Fierro, R., Lewis, F. L., 1997. Control of a Nonholonomic Mobile Robot: Backstepping Kinematics into Dynamics. *Journal of Robotic Systems*. Vol. 14, No. 3, pp. 149-163.
- Jeong, W., 2014. Performance Analysis of a Mobile Duct Cleaning Robot. *International Journal of Advanced Engineering Applications*. Vol. 7, No. 2, pp. 26-32.
- Kim, S., Jung, S., 2006. Hardware Implementation of a Neural Network Controller with an MCU and an FPGA for Nonlinear Systems. *International Journal of Control, Automation, and Systems*. Vol. 4, No. 5, pp. 567-574.
- Martinez, J. L., Mandow, A., Morales, A., Pedraza, S., Garcia-Cerezo, A., 2005. Approximating Kinematics for Tracked Mobile Robots. *The International Journal of Robotics Research*. Vol. 24, No. 10, pp. 867-878.
- King, M., 2010. *Process Control: A Practical Approach*. West Sussex: John Wiley and Son. pp. 36-50.
- Bloch, A. M., Reyhanoglu, M., McClamroch, N. H., 1992. Control and stabilization of nonholonomic dynamic systems. *IEEE Trans. Autom. Control*. Vol. 37, No. 11, pp. 1746-1757.
- Sarkar, N., Yun, X., Kumar, V., 1994. Control of mechanical systems with rolling constraints: Application to dynamic control of mobile robots. *Int. J. Rob. Res.* Vol. 13, No. 1, pp. 55-69.
- Yang, J. M., Kim, J. H., 1999. Sliding Mode Control for Trajectory Tracking of Nonholonomic Wheeled Mobile Robots. *IEEE Transactions on Robotics and Automation*. Vol. 15, No. 3, pp. 578-587.
- Kanayama, Y., Kimura, Y., Miyazaki, F., Noguchi, T., 1990. A stable tracking control method for an autonomous mobile robot. *IEEE International Conference on Robotics and Automation, 1990 May 13-18; Cincinnati, OH*. pp. 384-389.
- M'Closkey, R. T., Murray, R. M., 1994. Extending exponential stabilizers for nonholonomic systems from kinematic controllers to dynamic controllers. *Proc. IFAC Symp. Rob. Control, 1994; Capri, Italy*. pp. 211-216.